Asynchronous and Heterogeneous Track-to-Track Fusion with Mapped Process Noise and Cross-Covariance

KAIPEI YANG
YAAKOV BAR-SHALOM
PETER WILLETT

Track-to-track fusion has been studied extensively for both homogeneous and heterogeneous cases, these cases denoting common and disparate state models. However, as opposed to homogeneous fusion, the cross-covariance for heterogeneous local tracks (LTs) in different state spaces that accounts for the relationship between the process noises of the heterogeneous models seems not to be available in the literature. This work provides the derivation of the cross-covariance for heterogeneous LTs of different dimensions where the local states are related by a nonlinear transformation (with no inverse transformation). First, the relationship between the process noise covariances of the motion models in different state spaces is obtained. The cross-covariance of the local estimation errors is then derived in a recursive form by taking into account the relationship between the local state model process noises. Both the synchronous and asynchronous systems are considered. A linear minimum mean square fusion is carried out for a scenario involving tracks from two LTs: one from an active sensor and one from a passive sensor.

I. INTRODUCTION

In a heterogeneous system, the state models used by local sensors are in different state spaces with different dimensions. The fusion for heterogeneous systems needs investigation since it is closely related to the real-world problems. One reason for using distinct system models in the local trackers is the different sensor characteristics—active versus passive. For example, for self-driving vehicle system perception, heterogeneous tracks are inevitable due to different coordinate systems, which are related by a nonlinear transformation. Low-level fusion, or centralized track/fusion (CTF), is characterized by transferring raw data from each sensor to the fusion center (FC). It requires communication with high bandwidth since all the raw data need to be transferred on demand, which is not feasible for most of the practical applications. The track-to-track fusion (T2TF) to be considered is characterized by local tracking at each of the sensors and a fusion combining the tracks from multiple sensors at the FC. For several applications in defense systems and self-driving vehicle systems, T2TF fusion is preferred due to communication constraints.

For T2TF, it is critical to consider the cross-covariance between the track estimation errors of the same target at different local trackers. The fusion of homogeneous local tracks (LTs)—when the state models at two sensors are the same—considering the "common process noise" of the LTs is discussed in [1, Ch. 9]. The work [2] considered homogeneous T2TF with the cross-covariance for the asynchronous case. The fusion of heterogeneous LTs from local sensors that use different state models was presented in [3]; however, it assumed the cross-covariance between the local state estimation errors to be zero since the cross-covariance was not available. The contributions of this paper compared to [3] are as follows: (i) the cross-covariance of the process noises of the heterogeneous models is derived and (ii) the cross-covariance of the heterogeneous estimation errors from the LTs is derived. The recent work [4] deals with the heterogeneous T2TF in 3D using an infrared search and track (IRST) sensor and an air moving target indicator (MTI) radar based on information matrix fusion taking into account the cross-covariance between the LTs. However, the main limitation of [4] is that the authors assumed that the local state vectors have the same dimension with a unique inverse mapping, which is not realistic in most of the heterogeneous T2TF scenarios where the inverse transformation does not exist due to the different state space dimensions.

This work provides the derivation of the cross-covariance for the heterogeneous LTs of different dimensions where the local states are related by a nonlinear transformation without inverse transformation. The heterogeneous T2TF considered here has no information feedback. The relationship between the process noise covariances of the two motion models is presented. The state model process noise covariance

in the smaller state space can be obtained (through a mapping based on the nonlinear relationship) from the state model process noise covariance and the estimate in the larger state space. The cross-covariance of the estimation errors from two LTs is derived in a recursive form by taking into account the relationship between the local state model process noises. Both synchronous and asynchronous systems are considered. In the asynchronous case, where the sensors are having arbitrary sampling times, the fusion happens at the union of the sampling times of the two trackers, that is, with LT-driven communication. The asynchronous T2TF fusion is carried out for a scenario of two tracks of a single target (one from an active sensor and one from a passive sensor) with a linear minimum mean square (LMMSE) fuser in the simulation. The cross-correlation of the estimation errors is shown to be sometimes positive and sometimes negative depending on the sensor-trajectory geometry, which confirms the results in [3] from a Monte Carlo (MC) investigation.

The paper is organized as follows. Section II formulates the heterogeneous fusion problem and derives the relationship of the process noise covariances of the LT models. Section III presents the cross-covariance of the estimation errors. In Section IV, the state and measurement models for both the active sensor and passive sensor are introduced. Section V formulates the LMMSE fuser. Section VI presents the simulation results from MC runs. The summary and conclusions are provided in Section VII.

II. PROBLEM FORMULATION AND THE RELATIONSHIP BETWEEN THE PROCESS NOISES

A. Synchronous Case

In the synchronous case, the LTs share the same sampling time and are assumed to have the full rate communication with the FC. Consider the state models at sensors i and j in different state spaces with dimensions $n_{\mathbf{x}}^i$ and $n_{\mathbf{x}}^j$, respectively,

$$\mathbf{x}^i(k+1) = f^i[k, \mathbf{x}^i(k)] + \mathbf{v}^i(k), \tag{1}$$

$$\mathbf{x}^j(k+1) = f^j[k, \mathbf{x}^j(k)] + \mathbf{v}^j(k), \tag{2}$$

and the measurements of dimensions $n_{\mathbf{z}}^i$ and $n_{\mathbf{z}}^j$, respectively,

$$\mathbf{z}^i(k) = h^i[k, \mathbf{x}^i(k)] + \mathbf{w}^i(k), \tag{3}$$

$$\mathbf{z}^j(k) = h^j[k, \mathbf{x}^j(k)] + \mathbf{w}^j(k), \tag{4}$$

where $\mathbf{v}^m(k)$ and $\mathbf{w}^m(k), m = i, j$, are the process noises and measurement noises assumed to be additive, zero mean, and white with corresponding covariance matrices $Q^m(k)$ and $R^m(k)$ $(m = i, j)$. All the noises are also assumed to be mutually independent, except $\mathbf{v}^i$ is correlated with $\mathbf{v}^j$ since they pertain to the motion of the same

target, although in different state spaces. The recursion of the cross-covariance $Q^{ij}(k)$ between $\mathbf{v}^i(k)$ and $\mathbf{v}^j(k)$ will be discussed later.

The nonlinear functions $f^m[\cdot, \cdot]$ and $h^m[\cdot, \cdot], m = i, j$, are distinct and may be time varying. The two state vectors have a nonlinear relationship[1]

$$\mathbf{x}^j = \alpha\left[\mathbf{x}^i\right]; \tag{5}$$

with $n_{\mathbf{x}}^i > n_{\mathbf{x}}^j$, it is clear that (5) has no inverse.

Substituting (1) into the above equation yields

$$\mathbf{x}^j(k+1) = \alpha\left[\mathbf{x}^i(k+1)\right] = \alpha\left[f^i[k, \mathbf{x}^i(k)] + \mathbf{v}^i(k)\right]. \tag{6}$$

The vector Taylor series expansion of (6) up to the first-order term is

$$\alpha\left[\mathbf{x}^i(k+1)\right] = \alpha\left[f^i[k, \mathbf{x}^i(k)]\right]$$
$$+ [\nabla_x \alpha(x)']'|_{x=f^i[k,\mathbf{x}^i(k)]}\mathbf{v}^i(k). \tag{7}$$

Thus,

$$\mathbf{v}^j(k) \approx [\nabla_x \alpha(x)']'|_{x=f^i[k,\mathbf{x}^i(k)]}\mathbf{v}^i(k) = A(k)\mathbf{v}^i(k), \tag{8}$$

where

$$A(k) \triangleq [\nabla_x \alpha(x)']'|_{x=f^i[k,\mathbf{x}^i(k)]} \tag{9}$$

is the $(n_{\mathbf{x}}^j \times n_{\mathbf{x}}^i$, i.e., not square) Jacobian corresponding to (8).

Then, $Q^j(k)$, the covariance of the process noise $v^j(k)$, can be expressed using $Q^i(k)$ as follows:

$$Q^j(k) = E\left[\mathbf{v}^j(k)\mathbf{v}^j(k)'\right] = A(k)Q^i(k)A(k)', \tag{10}$$

and the cross-covariance between the two process noises is

$$Q^{ij}(k) = E\left[\mathbf{v}^i(k)\mathbf{v}^j(k)'\right] = Q^i(k)A(k)'. \tag{11}$$

Note that in the estimation problem where the state is not available, the Jacobian (9) will have to be evaluated at the latest estimate.

B. Asynchronous Case

With LT (local filter/tracker)-driven communication, the fusion of an asynchronous system (i.e., with tracks from radar and infrared/electro-optical sensors) is carried out whenever the FC receives new information. As shown in Fig. 1, sensor i is assumed to be the active one with state vector in the larger state space (of dimension $n_{\mathbf{x}}^i$) and sensor j is the passive one with state vector in the smaller state space (of dimension $n_{\mathbf{x}}^j, n_{\mathbf{x}}^j < n_{\mathbf{x}}^i$). For the FC, the fusion times are equal to the times when new information is obtained. From this figure, we have

$$t_{k+1} = t_{m+1}^j \tag{12}$$

---

[1]This is in general, and subsumes cases of equivalent states, situations in which one state is a subset of the other, and other more complicated relationships.
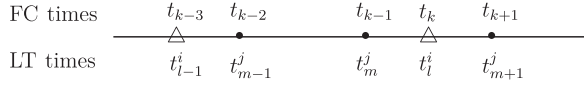
| FC times | t_{k-3} | t_{k-2} | | t_{k-1} | t_k | t_{k+1} |
| LT times | t_{l-1}^i | t_{m-1}^j | | t_m^j | t_l^i | t_{m+1}^j |

Fig. 1. FC times and LT times in asynchronous T2TF.

and

$$t_k = t_l^i, \tag{13}$$

where l and m denote the respective LT sampling indices.

Since the state error cross-covariance will have to be iterated according to the FC times[2]

$$\{t_k\} = \{t_l^i\} \bigcup \{t_m^j\}, \tag{14}$$

we will develop the relationship between the process noises of the different local states

$$f^j[t_{k+1}, t_k, \mathbf{x}^j(t_k)] + \mathbf{v}^j(t_{k+1}, t_k)$$
$$= \alpha \left[f^i[t_{k+1}, t_k, \mathbf{x}^i(t_k)] + \mathbf{v}^i(t_{k+1}, t_k) \right]. \tag{15}$$

Different from the synchronous case, the nonlinear functions $f^i[\cdot, \cdot, \cdot]$ and $f^j[\cdot, \cdot, \cdot]$ have three arguments: propagation end time, propagation start time, and the state at the propagation start time. The process noises $\mathbf{v}^i(\cdot, \cdot)$ and $\mathbf{v}^j(\cdot, \cdot)$ have two arguments: propagation end time and propagation start time. Following (7) with first-order Taylor expansion, the second term on the left-hand side is given by

$$\mathbf{v}^j(t_{k+1}, t_k) = A(t_k)\mathbf{v}^i(t_{k+1}, t_k), \tag{16}$$

where

$$A(t_k^i) \triangleq \left[\nabla_x \alpha(x)' \right]' \Big|_{x = f^i[t_{k+1}, t_k, \mathbf{x}^i(t_k)]} \tag{17}$$

with dimension $n^j \times n^i$.

The covariance matrix of $\mathbf{v}^j(t_{k+1}, t_k)$ can be obtained by

$$Q^j(t_{k+1}, t_k) \triangleq E[\mathbf{v}^j(t_{k+1}, t_k)\mathbf{v}^j(t_{k+1}, t_k)']$$
$$= E[A(t_k)\mathbf{v}^i(t_{k+1}, t_k)\mathbf{v}^i(t_{k+1}, t_k)'A(t_k)']$$
$$= A(t_k)Q^i(t_{k+1}, t_k)A(t_k)'. \tag{18}$$

The cross-covariance between the process noises is

$$Q^{ij}(t_{k+1}, t_k) \triangleq E[\mathbf{v}^i(t_{k+1}, t_k)\mathbf{v}^j(t_{k+1}, t_k)']$$
$$= E[\mathbf{v}^i(t_{k+1}, t_k)\mathbf{v}^i(t_{k+1}, t_k)'A(t_k)']$$
$$= Q^i(t_{k+1}, t_k)A(t_k)'. \tag{19}$$

The process noises are assumed to be additive, zero mean, and white. It should be noted that to ensure the whiteness of the discrete time process noises over the arbitrary sampling intervals, one has to use the discretized continuous-time white noise state propagation models.

___

[2]For asynchronous homogeneous sensors (with same LT states), the cross-covariance iteration is given in [1, eq. (9.3.2-5)] based on the "common process noise." This has to be generalized to the heterogeneous states where there is no common process noise but the process noises in the different states models are related.

III. THE CROSS-COVARIANCE OF THE ESTIMATION ERRORS

A. Synchronous Case

Consider a tracker at a single sensor (this could be sensor i or sensor j) with the state model and measurement model to be

$$\mathbf{x}(k+1) = f[k, \mathbf{x}(k)] + \mathbf{v}(k), \tag{20}$$

$$\mathbf{z}(k+1) = h[k, \mathbf{x}(k)] + \mathbf{w}(k). \tag{21}$$

The updated state at time k is, using an extended Kalman filter (EKF),

$$\hat{\mathbf{x}}(k|k) = f[\hat{\mathbf{x}}(k-1|k-1)] + W(k)\nu(k). \tag{22}$$

Expanding $h[k, \mathbf{x}(k)]$ around $\hat{\mathbf{x}}(k|k-1)$ yields the innovation

$$\nu(k) = h[k, \mathbf{x}(k)] + \mathbf{w}(k) - h[k, \hat{\mathbf{x}}(k|k-1)]$$
$$= h[k, \hat{\mathbf{x}}(k|k-1)] + H(k)[\mathbf{x}(k) - \hat{\mathbf{x}}(k|k-1)]$$
$$\quad + \mathbf{w}(k) - h[k, \hat{\mathbf{x}}(k|k-1)]$$
$$= H(k)[\mathbf{x}(k) - \hat{\mathbf{x}}(k|k-1)] + \mathbf{w}(k), \tag{23}$$

where

$$H(k) = \left[\nabla_x h(k, x)' \right]' \Big|_{x = \hat{\mathbf{x}}(k|k-1))}. \tag{24}$$

Using the dynamic equation (20), (23) can be written as

$$\nu(k) = H(k)\{f[\mathbf{x}(k-1)] + \mathbf{v}(k-1)$$
$$\quad - f[\hat{\mathbf{x}}(k-1|k-1))]\} + \mathbf{w}(k). \tag{25}$$

Expanding $f[\mathbf{x}(k-1)]$ around $\hat{\mathbf{x}}(k-1|k-1)$ yields

$$\nu(k) = H(k)\{f[\hat{\mathbf{x}}(k-1|k-1)] + F(k-1)[\mathbf{x}(k-1)$$
$$\quad - \hat{\mathbf{x}}(k-1|k-1)] + \mathbf{v}(k-1)$$
$$\quad - f[\hat{\mathbf{x}}(k-1|k-1)]\} + \mathbf{w}(k)$$
$$= H(k)F(k-1)\tilde{\mathbf{x}}(k-1|k-1)$$
$$\quad + H(k)\mathbf{v}(k-1) + \mathbf{w}(k), \tag{26}$$

where

$$F(k-1) = \left[\nabla_x f(k-1, x)' \right]' \Big|_{x = \hat{\mathbf{x}}(k-1|k-1)}. \tag{27}$$

The estimation error at time $k-1$ is

$$\tilde{\mathbf{x}}(k-1|k-1) = \mathbf{x}(k-1) - \hat{\mathbf{x}}(k-1|k-1). \tag{28}$$

Substituting (26) into (22) yields

$$\hat{\mathbf{x}}(k|k) = f[\hat{\mathbf{x}}(k-1|k-1)]$$
$$\quad + W(k)[H(k)F(k-1)\tilde{\mathbf{x}}(k-1|k-1)$$
$$\quad + H(k)\mathbf{v}(k-1) + \mathbf{w}(k)]. \tag{29}$$

The first-order vector Taylor series expansion of (20) around $\hat{\mathbf{x}}(k-1|k-1)$ is

$$\mathbf{x}(k) = f[\hat{\mathbf{x}}(k-1|k-1)] + F(k-1)\tilde{\mathbf{x}}(k-1|k-1) + \mathbf{v}(k-1). \tag{30}$$

Subtracting (29) from (30), the estimation error at time k can be expressed as

$$\tilde{\mathbf{x}}(k|k) = \mathbf{x}(k) - \hat{\mathbf{x}}(k|k)$$
$$= [I_{n_{\mathbf{x}}} - W(k)H(k)]F(k-1)\tilde{\mathbf{x}}(k-1|k-1)$$
$$+ [I_{n_{\mathbf{x}}} - W(k)H(k)]\mathbf{v}(k-1) + W(k)\mathbf{w}(k), \quad (31)$$

where $I_{n_{\mathbf{x}}}$ is the $n_{\mathbf{x}}$-dimensional identity matrix and $n_{\mathbf{x}}$ is the dimension of the state vector $\mathbf{x}$.

Following the discussion above, the estimation errors from the two sensors i and j are

$$\tilde{\mathbf{x}}^i(k|k) = \mathbf{x}^i(k) - \hat{\mathbf{x}}^i(k|k)$$
$$= [I_{n_{\mathbf{x}}^i} - W^i(k)H^i(k)]F^i(k-1)\tilde{\mathbf{x}}^i(k-1|k-1)$$
$$+ [I_{n_{\mathbf{x}}^i} - W^i(k)H^i(k)]\mathbf{v}^i(k-1) + W^i(k)\mathbf{w}^i(k), \quad (32)$$

$$\tilde{\mathbf{x}}^j(k|k) = \mathbf{x}^j(k) - \hat{\mathbf{x}}^j(k|k)$$
$$= h[\mathbf{x}^i(k)] - \hat{\mathbf{x}}^j(k|k)$$
$$= [I_{n_{\mathbf{x}}^j} - W^j(k)H^j(k)]F^j(k-1)\tilde{\mathbf{x}}^j(k-1|k-1)$$
$$+ [I_{n_{\mathbf{x}}^j} - W^j(k)H^j(k)]\mathbf{v}^j(k-1) + W^j(k)\mathbf{w}^j(k). \quad (33)$$

Note that $\mathbf{x}^j(k)$ in (33) is $\alpha[\mathbf{x}^i(k)]$ (5); that is, there is a common truth in (32) and (33).

Then, the estimation errors' cross-covariance (of dimension $n_{\mathbf{x}}^i \times n_{\mathbf{x}}^j$) is

$$P^{ij}(k|k) = E[\tilde{\mathbf{x}}^i(k|k)\tilde{\mathbf{x}}^j(k|k)']$$
$$= [I - W^i(k)H^i(k)]F^i(k-1)P^{ij}(k-1|k-1)$$
$$\times F^j(k-1)'[I - W^j(k)H^j(k)]'$$
$$+ [I - W^i(k)H^i(k)]Q^{ij}(k-1)[I - W^j(k)H^j(k)]'$$
$$= [I - W^i(k)H^i(k)]\{F^i(k-1)P^{ij}(k-1|k-1)F^j(k-1)'$$
$$+ Q^{ij}(k-1)\}[I - W^j(k)H^j(k)]'. \quad (34)$$

B. Asynchronous Case

In this case, the cross-covariance between the estimation errors is, based on [1, eq. (9.3.2-5)] and the previous discussion about the synchronous case,

$$P^{ij}(t_k|t_k) = [I - \chi^i(t_k)W^i(t_k)H^i(t_k)]$$
$$\cdot \{F^i(t_k, t_{k-1}, \hat{\mathbf{x}}^i(t_{k-1}|t^i(t_{k-1})))P^{ij}(t_{k-1}|t_{k-1})$$
$$\times F^j(t_k, t_{k-1}, \hat{\mathbf{x}}^j(t_{k-1}|t^j(t_{k-1})))'$$
$$+ Q^{ij}(t_k, t_{k-1})\}[I - \chi^j(t_k)W^j(t_k)H^j(t_k)]', \quad (35)$$

where $t^i(t_{k-1})$ and $t^j(t_{k-1})$ are the most recent times prior to t_{k-1} at which LT i and LT j sent information to the FC,

respectively, and

$$F^i(t_k, t_{k-1}, \hat{\mathbf{x}}^i(t_{k-1}|t^i(t_{k-1})))$$
$$= [\nabla_x f^i(t_k, t_{k-1}, x)']' |_{x=\hat{\mathbf{x}}^i(t_{k-1}|t^i(t_{k-1}))}, \quad (36)$$

$$F^j(t_k, t_{k-1}, \hat{\mathbf{x}}^j(t_{k-1}|t^j(t_{k-1})))$$
$$= [\nabla_x f^j(t_k, t_{k-1}, x)']' |_{x=\hat{\mathbf{x}}^j(t_{k-1}|t^j(t_{k-1}))}. \quad (37)$$

In (35),

$$\chi^i(t_k) = \begin{cases} 1, & \text{if sensor } i \text{ has a measurement at time } t_k, \\ 0, & \text{others,} \end{cases} \quad (38)$$

similarly for sensor j.

With the following assumptions for the previous fused estimate $\hat{\mathbf{x}}(t_{k-1}|t_{k-1})$:

$$F^i(t_k, t_{k-1}, \hat{\mathbf{x}}^i(t_{k-1}|t^i(t_{k-1}))) \approx F^i(t_k, t_{k-1}, \hat{\mathbf{x}}(t_{k-1}|t_{k-1})), \quad (39)$$

$$F^j(t_k, t_{k-1}, \hat{\mathbf{x}}^j(t_{k-1}|t^j(t_{k-1}))) \approx F^j(t_k, t_{k-1}, \hat{\mathbf{x}}(t_{k-1}|t_{k-1})), \quad (40)$$

equation (35) becomes

$$P^{ij}(t_k|t_k) = [I - \chi^i(t_k)W^i(t_k)H^i(t_k)]$$
$$\cdot \{F^i(t_k, t_{k-1}, \hat{\mathbf{x}}(t_{k-1}|t_{k-1}))P^{ij}(t_{k-1}|t_{k-1})$$
$$\times F^j(t_k, t_{k-1}, \hat{\mathbf{x}}(t_{k-1}|t_{k-1}))'$$
$$+ Q^{ij}(t_k, t_{k-1})\}[I - \chi^j(t_k)W^j(t_k)H^j(t_k)]'. \quad (41)$$

If the fusion is at a time when there is an updated state only from LT$_i$, it will use a prediction to that time from LT$_j$. Note that although the fusion can be carried out on demand, the cross-covariance calculation needs to run with full rate.

IV. THE STATE MODELS FOR THE ACTIVE AND PASSIVE SENSORS

In the ξ–η space, an active sensor located at $[\xi^{\mathrm{a}} \; \eta^{\mathrm{a}}]$ with range and azimuth angle measurements (without time arguments, for simplicity)

$$r = \sqrt{(\xi - \xi^{\mathrm{a}})^2 + (\eta - \eta^{\mathrm{a}})^2} + w^{\mathrm{r}}, \quad (42)$$

$$\theta^{\mathrm{a}} = \tan^{-1}[(\eta - \eta^{\mathrm{a}})/(\xi - \xi^{\mathrm{a}})] + w^{\mathrm{a}} \quad (43)$$

and a passive sensor located at $[\xi^{\mathrm{p}} \; \eta^{\mathrm{p}}]$ with bearing measurements only

$$\theta^{\mathrm{p}} = \tan^{-1}[(\eta - \eta^{\mathrm{p}})/(\xi - \xi^{\mathrm{p}})] + w^{\mathrm{p}} \quad (44)$$

are considered for the T2TF for a 2D target. The measurement noises w^{r}, w^{a}, and w^{p} are assumed to be independent zero-mean white Gaussian with corresponding standard deviations σ^{r}, σ^{a}, and σ^{p}.

The active sensor's measurements in polar coordinates are transformed into Cartesian coordinates with an unbiased transformation [5, Sec. 10.4.3]. Given (42) and (43), the unbiased transformed measurement vector is

$$\mathbf{z}^{C} = \begin{bmatrix} \xi^{C} \\ \eta^{C} \end{bmatrix} = \begin{bmatrix} b_1^{-1} r \cos(\theta^{a}) + \xi^{a} \\ b_1^{-1} r \sin(\theta^{a}) + \eta^{a} \end{bmatrix}, \qquad (45)$$

where

$$b_1 = e^{-\sigma^{a}/2}. \qquad (46)$$

The transformed active sensor noise vector $\mathbf{w}_C$ has the covariance matrix $\mathbf{R}_C$ with elements

$$\mathbf{R}_C(1,1) = b_1^{-2} r^2 \cos(\theta^{a}) + 0.5(r^2 + \sigma^{a})(1 + b_1^4 \cos(\theta^{a})), \qquad (47)$$

$$\mathbf{R}_C(2,2) = b_1^{-2} r^2 \sin(\theta^{a}) + 0.5(r^2 + \sigma^{a})(1 - b_1^4 \cos(\theta^{a})), \qquad (48)$$

$$\begin{aligned} \mathbf{R}_C(1,2) &= \mathbf{R}_C(2,1) \\ &= (0.5 b_1^{-2} r^2 + 0.5(r^2 + \sigma^{a}) b_1^4 - r^2) \sin(2\theta^{a}). \end{aligned} \qquad (49)$$

For the active sensor, a nearly coordinated turn model [7] is used for tracking along with an EKF. The 5D state vector[3] includes position, velocity, and turn rate Ω, that is,

$$\mathbf{x}^{a} = [\xi \ \dot{\xi} \ \eta \ \dot{\eta} \ \Omega] \qquad (50)$$

with the discretized dynamic model to be

$$\mathbf{x}^{a}(t_{l+1}^{a}) = f^{a}[\mathbf{x}^{a}(t_l^{a})] + \mathbf{v}^{a}[\mathbf{x}^{a}(t_l^{a})], \qquad (51)$$

$$\mathbf{z}^{C} = H^{a} \mathbf{x}^{a}(t_l^{a}) + \mathbf{w}^{C}(t_l^{a}), \qquad (52)$$

where

$$f^{a}[\mathbf{x}^{a}(t_l^{a})]$$
$$= \begin{bmatrix} \xi(t_l^{a}) + T^{a}\dot{\xi}(t_l^{a}) - (T^{a})^2 \Omega(t_l^{a})\dot{\eta}(t_l^{a})/2 \\ \dot{\xi}(t_l^{a}) - T^{a}\Omega(t_l^{a})\dot{\eta}(t_l^{a}) - (T^{a})^2 \Omega(t_l^{a})^2 \dot{\xi}(t_l^{a})/2 \\ \eta(t_l^{a}) + T^{a}\dot{\eta}(t_l^{a}) + (T^{a})^2 \Omega(t_l^{a})\dot{\xi}(t_l^{a})/2 \\ \dot{\eta}(t_l^{a}) + T^{a}\Omega(t_l^{a})\dot{\xi}(t_l^{a}) - (T^{a})^2 \Omega(t_l^{a})^2 \dot{\eta}(t_l^{a})/2 \\ \Omega(t_l^{a}) \end{bmatrix}, \qquad (53)$$

$$H^{a} = \begin{bmatrix} 1 & 0 & 0 & 0 & 0 \\ 0 & 0 & 1 & 0 & 0 \end{bmatrix}. \qquad (54)$$

The process noise vector is target state dependent and its covariance matrix is discussed in [3]. The continuous-time process noise "intensities" are the power spectral densities that need to be chosen in the design of the process noise covariance matrix.

The passive sensor uses a Kalman filter based on a continuous-time Wiener process acceleration model with a state vector involving the angle, angle rate, and angle acceleration:

$$\mathbf{x}^{p} = [\theta \ \dot{\theta} \ \ddot{\theta}]. \qquad (55)$$

The discretized dynamic model is

$$\mathbf{x}^{p}(t_m^{p} + 1) = F^{p} \mathbf{x}^{p}(t_m^{p}) + \mathbf{v}^{p}(t_m^{p}), \qquad (56)$$

$$\mathbf{z}^{p} = H^{p} \mathbf{x}^{p}(t_m^{p}) + \mathbf{w}^{p}(t_m^{p}), \qquad (57)$$

where

$$F^{p} = \begin{bmatrix} 1 & T^{p} & (T^{p})^2/2 \\ 0 & 1 & T^{p} \\ 0 & 0 & 1 \end{bmatrix}, \qquad (58)$$

$$H^{p} = \begin{bmatrix} 1 & 0 & 0 \end{bmatrix}. \qquad (59)$$

The process noise covariance matrix of the passive tracker's model at time k has the relationship with active process noise covariance matrix shown in (10). The state vector (50) and the state vector (55) have a nonlinear relationship

$$\mathbf{x}^{p} = \alpha [\mathbf{x}^{a}] \qquad (60)$$

with explicit expressions

$$\theta = \text{atan}\left(\frac{\eta - \eta^{p}}{\xi - \xi^{p}}\right), \qquad (61)$$

$$\dot{\theta} = \frac{v \sin(\phi)}{r^{p}}, \qquad (62)$$

$$\ddot{\theta} = \frac{v \cos(\phi)\Omega}{r^{p}}, \qquad (63)$$

where v is the target speed

$$v = \sqrt{\dot{\xi}^2 + \dot{\eta}^2}, \qquad (64)$$

r^{p} is the range with respect to the passive sensor's location

$$r^{p} = \sqrt{(\xi - \xi^{p})^2 + (\eta - \eta^{p})^2}, \qquad (65)$$

and ϕ is the difference between velocity angle and position azimuth angle:

$$\phi = \text{atan}\left(\frac{\dot{\eta}}{\dot{\xi}}\right) - \text{atan}\left(\frac{\eta - \eta^{p}}{\xi - \xi^{p}}\right). \qquad (66)$$

V. THE LMMSE ESTIMATOR FOR HETEROGENEOUS T2TF

A. Synchronous Case

The LMMSE estimation for heterogeneous T2TF is carried out (omitting the time arguments) with

$$\hat{\mathbf{x}}^{i} = \hat{\mathbf{x}}^{a}(1:4) = [\hat{\xi} \ \hat{\dot{\xi}} \ \hat{\eta} \ \hat{\dot{\eta}}]' \qquad (67)$$

---

[3]Here, the superscripts i and j used in the previous text are replaced by "a" and "p" to indicate the states are from one active sensor and one passive sensor, respectively.

as the active sensor's track and

$$\hat{\mathbf{x}}^j = \hat{\mathbf{x}}^p(1:2) = [\hat{\theta}\ \ \hat{\dot{\theta}}]' \qquad (68)$$

as the passive sensor's track.

The fused track estimate is obtained by (derivation can be found in [1, Sec. 9.2.3])

$$\hat{\mathbf{x}}^i_{\text{LMMSE}} = \hat{\mathbf{x}}^i + P_{\mathbf{xz}}P_{\mathbf{zz}}^{-1}[\hat{\mathbf{x}}^j - g[\hat{\mathbf{x}}^i]], \qquad (69)$$

where $g[\cdot]$ is the nonlinear relationship between the states from the two sensors. Here, we use g rather than α to avoid ambiguity in calculating the different Jacobians. The corresponding fused covariance matrix is

$$P^i_{\text{LMMSE}} = P^i - P_{\mathbf{xz}}P_{\mathbf{zz}}^{-1}P'_{\mathbf{xz}}, \qquad (70)$$

where

$$P_{\mathbf{xz}} \approx P^i(G^i)' - P^{ij}, \qquad (71)$$

$$P_{\mathbf{zz}} \approx P^i - G^i P^{ij} - P^{ji}(G^i)' + G^i P^i(G^i)', \qquad (72)$$

and

$$G^i = [\nabla^i_{\mathbf{x}}g(\mathbf{x}^j)']'|_{\mathbf{x}^i=\hat{\mathbf{x}}^i} \qquad (73)$$

is the Jacobian evaluated at the estimate from sensor i.

B. Asynchronous Case

In the asynchronous case, the fusion is carried out at the times given by the union of the different sampling times of the two sensors. Since not all the LTs' communications are available to the FC at the fusion time, predictions of the LTs' latest estimates (prior or at the fusion time) are used for LMMSE estimation. The fused track estimate (extension of (69)) at time t_k is obtained by

$$\hat{\mathbf{x}}_{\text{LMMSE}}(t_k) = f^i\left[t_k, t^i(t_k), \hat{\mathbf{x}}^i[t^i(t_k)|t^i(t_k)]\right]$$
$$+ P_{\mathbf{xz}}P_{\mathbf{xz}}^{-1}\Big\{ f^j\left[t_k, t^j(t_k), \hat{\mathbf{x}}^j[t^j(t_k)|t^j(t_k)]\right]$$
$$- g\Big[f^i\left[t_k, t^i(t_k), \hat{\mathbf{x}}^i[t^i(t_k)|t^i(t_k)]\right]\Big]\Big\}, \quad (74)$$

where $t^i(t_k)$ and $t^j(t_k)$ are the latest times up to and including t_k at which LT i and LT j sent information to the FC. In (74), the latest estimates (or the predication if needed) are used. The corresponding fused covariance matrix calculation is carried out (based on (70)) in terms of the LTs' latest covariance matrices

$$P^i_{\text{LMMSE}}(t_k) = P^i(t_k|t^i(t_k)) - P_{\mathbf{xz}}P_{\mathbf{zz}}^{-1}P'_{\mathbf{xz}}, \qquad (75)$$

where

$$P_{\mathbf{xz}} \approx P^i(t_k|t^i(t_k))G^i(t_k|t^i(t_k))' - P^{ij}(t_k|t_k), \qquad (76)$$

$$P_{\mathbf{zz}} \approx P^j(t_k|t^i(t_k)) - G^i(t_k|t^i(t_k))P^{ij}(t_k|t_k)$$
$$- P^{ji}(t_k|t_k)G^i(t_k|t^i(t_k))'$$
$$+ G^i(t_k|t^i(t_k))P^i(t_k|t^i(t_k))G^i(t_k|t^i(t_k))', \quad (77)$$

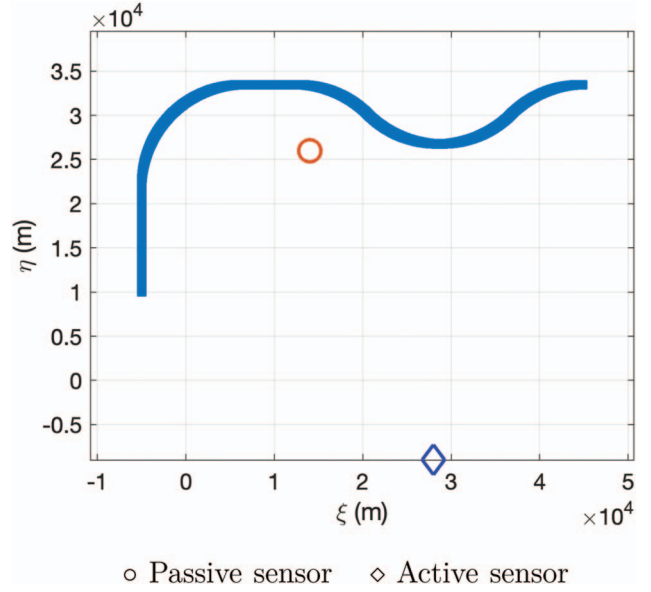o Passive sensor   ◇ Active sensor

Fig. 2. Target trajectory on the ξ–η plane.

and

$$G^i(t_k|t^i(t_k)) = [\nabla^i_{\mathbf{x}}g(\mathbf{x}^j)']'|_{\mathbf{x}^i=f^i\left[t_k, t^i(t_k), \hat{\mathbf{x}}^i[t^i(t_k)|t^i(t_k)]\right]} \quad (78)$$

is the Jacobian evaluated at the prediction/estimate from LT i. The covariance matrix from LT i is

$$P^i(t_k|t^i(t_k))$$
$$= \begin{cases} P^i(t^i(t_k)|t^i(t_k)), & \text{if } t_k = t^i(t_k), \\ F^i\left[t_k, t^i(t_k), \hat{\mathbf{x}}^i[t^i(t_k)|t^i(t_k)]\right]P^i(t^i(t_k)|t^i(t_k)) \\ \quad \cdot F^i\left[t_k, t^i(t_k), \hat{\mathbf{x}}^i[t^i(t_k)|t^i(t_k)]\right]' + Q^i(t_k, t^i(t_k)), & \text{others.} \end{cases}$$
$$(79)$$

VI. SIMULATION RESULTS

In the simulation, a target moving in a plane is considered with initial position $[-5\ 10]$ km and the initial velocity $[0\quad 200]$ m/s in Cartesian coordinates. The tar-
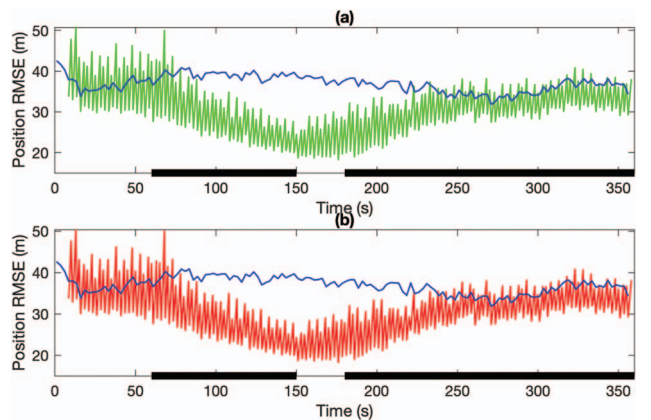
(a) — Active sensor   — Fusion without cross-covariance

(b) — Active sensor   — Fusion with cross-covariance

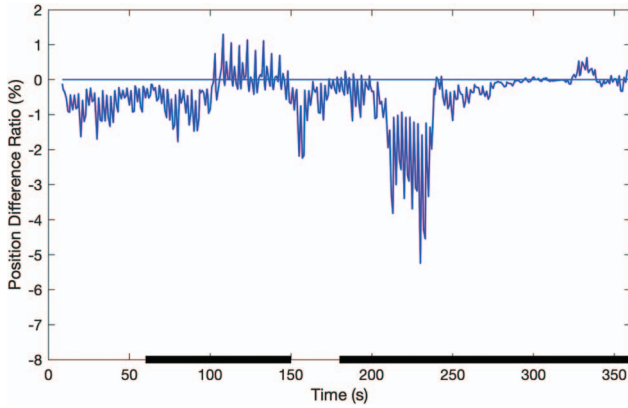Fig. 3. Position RMSEs from 500 MC runs.

Fig. 4. Position RMSE difference ratio of the fused estimate (with cross-covariance minus without cross-covariance divided by without cross-covariance).
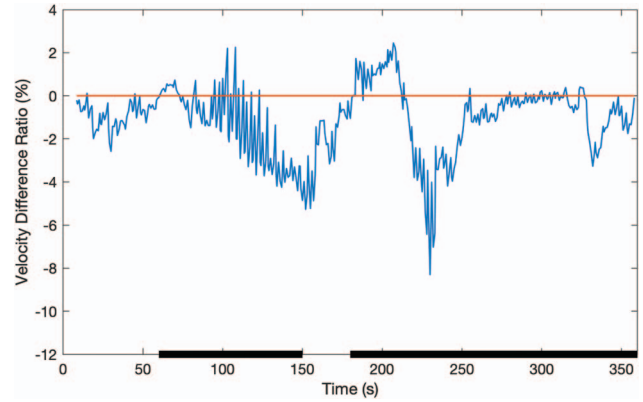

Fig. 6. Velocity RMSE difference ratio of the fused estimate (with cross-covariance minus without cross-covariance divided by without cross-covariance).

get keeps going straight for 60 s and makes a right turn at 1 rad/s for 90 s. Then, it keeps straight for another 30 s and turns to the right with turn rate 1 rad/s lasting for 45 s, followed by a left turn at 1 rad/s for 90 s, and finally makes a right turn at 1 rad/s for 45 s. The trajectory of the target is shown in Fig. 2.

The active sensor is located at $[28 \ {-}9]$ km with measurement noise standard deviations $\sigma^{\mathrm{r}} = 20$ m and $\sigma^{\mathrm{a}} = 1$ mrad. The passive sensor is located at $[14 \quad 26]$ km with angle measurement noise $\sigma^{\mathrm{p}} = 1$ mrad. The sampling intervals are $T^{\mathrm{a}} = 2.5$ s (for the active sensor) and $T^{\mathrm{p}} = 1$ s (for the passive sensor). Five hundred MC runs are made in the simulation to obtain the results. Maneuver duration is highlighted on the time axis in the following figures.

Fig. 3 shows the root mean square errors (RMSEs) of the position vector from the active sensor, for both fusion without cross-covariance and fusion with cross-covariance. The difference ratio between the latter two is compared (RMSE of fusion with cross-covariance minus RMSE of fusion without cross-covariance divided by the latter one) in Fig. 4. Similarly, the velocity vec-

tor RMSEs are shown in Fig. 5 with the difference comparison shown in Fig. 6. The negative differences shown in Figs. 3 and 5 indicate better performance of the fusion with cross-covariance as it achieves smaller RMSE. For position, the fusion with cross-covariance has RMSE reduction up to 6% (MSE reduction 12%); for velocity, the fusion with cross-covariance has RMSE reduction up to 8% (MSE reduction 16%). The difference ratio depends on the maneuvers but is not only limited to that since the maneuvers are not obvious to the passive sensor. The performance is sensitive to the geometry of the target's trajectory and the sensor positions. The CTF using the original measurements sequentially from different sensors is compared with the proposed fusion approach with simulation results shown in Figs. 7 and 8 for position and velocity, respectively. As shown in [3], the CTF using interacting multiple model (IMM) cannot "see" the maneuvers at the times when there is only a passive sensor measurement—the CTF IMM performs worse than the heterogeneous T2TF. For the case considered in this work, the FC used one EKF only. The CTF is sometimes worse (e.g., when the target starts maneuvering after 60 s) since the passive measurements (angle only) used in CTF-EKF cannot
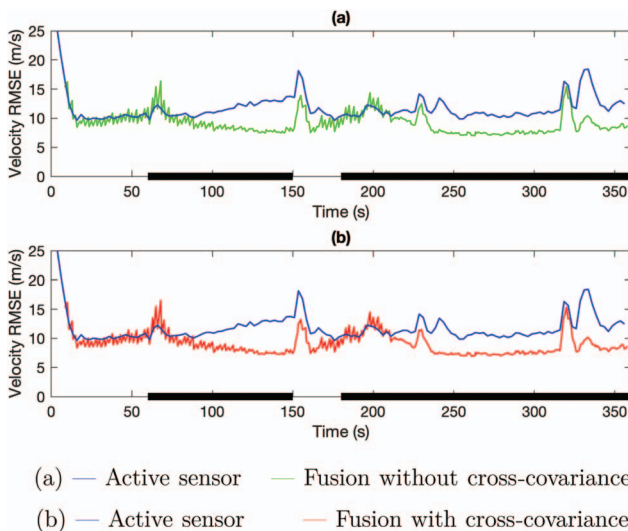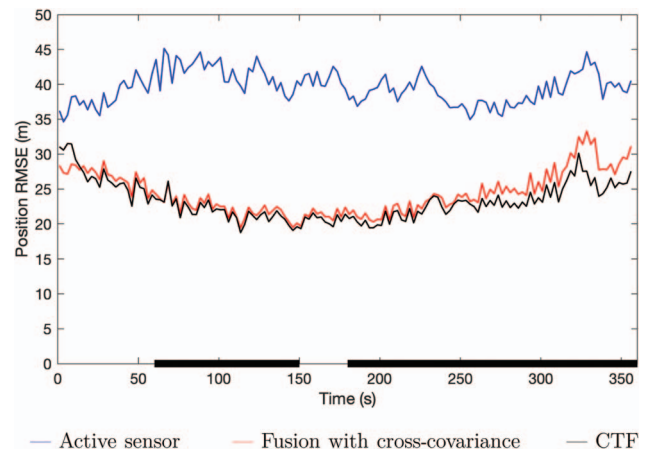

(a) — Active sensor   — Fusion without cross-covariance

(b) — Active sensor   — Fusion with cross-covariance

Fig. 5. Velocity RMSEs from 500 MC runs.

— Active sensor   — Fusion with cross-covariance   — CTF

Fig. 7. Position RMSEs of the fused estimate.

Fig. 8.   Velocity RMSEs of the fused estimate.

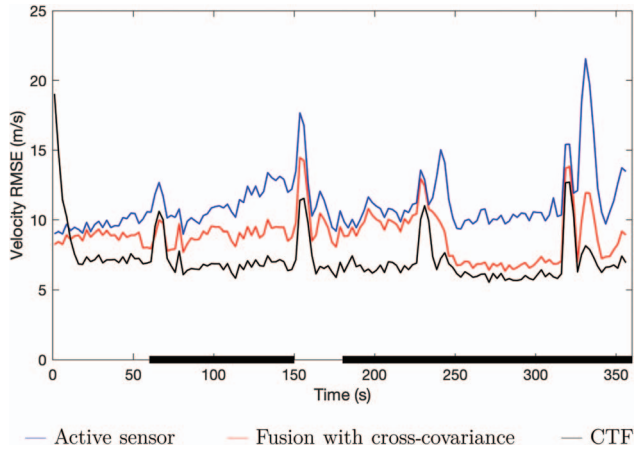Fig. 10.   NEES from 500 runs.

provide sufficient information on the target's velocity and maneuvers. The IMM is not used at the FC since the cross-covariance needs to be weighted based on the model probabilities and the relationship of different state models in Cartesian space and in angle space. In this work, this information is not available at the FC.

For the asynchronous, heterogeneous, and nonlinear case considered, the fusion with cross-covariance yields the actual variance, which is sometimes larger and sometimes smaller than the variance obtained under the (inaccurate) assumption of independence between the estimation errors. The variance differences (variance of fusion with cross-covariance minus variance of fusion without cross-covariance) for each component in the Cartesian state vector are shown in Fig. 9. Neglecting the cross-covariance between the estimation errors makes the fusion sometimes optimistic and sometimes pessimistic. The normalized estimation error squared (NEES) with the maneuver duration highlighted is shown in Fig. 10. Due to the facts that (i) the target is maneuvering (i.e., its motion uncertainty is deterministic rather than a stochastic white noise process) and (ii) the local trackers are running asynchronously, the system is not expected to be consistent with the ideal NEES of 4. For the white noise-driven motion model as
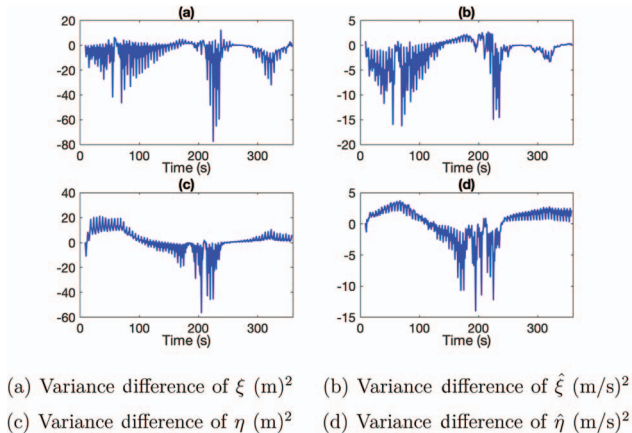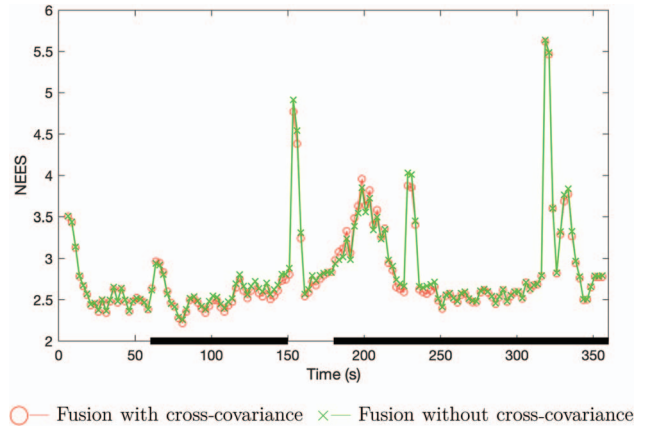
in [6], the fusion with cross-covariance was shown to be consistent.

The cross-correlation coefficients between the elements in (67) and (68) are shown in Fig. 11. The cross-correlation coefficients depend on the geometry of the two sensors and the target as well as the maneuvers of the target. It can be seen from Fig. 9 that some of the cross-correlation coefficients are positive and some of them are negative. This confirms the results in [3], which were obtained numerically through an MC investigation.

VII.   SUMMARY AND CONCLUSIONS

In this work, we derived the cross-covariance (for both the synchronous and asynchronous cases) between the local estimation errors of heterogeneous tracks from local sensors with different state models. The simulation

(a) Variance difference of ξ (m)^2 (b) Variance difference of $\hat{\xi}$ (m/s)^2

(c) Variance difference of η (m)^2 (d) Variance difference of $\hat{\eta}$ (m/s)^2

Fig. 9.   Variance difference of elements from the state vector in Cartesian coordinates.

(a)   — $\hat{\xi}$ and $\hat{\theta}$ — $\hat{\eta}$ and $\hat{\theta}$

(b)   — $\hat{\xi}$ and $\hat{\dot{\theta}}$ — $\hat{\eta}$ and $\hat{\dot{\theta}}$

(c)   — $\hat{\dot{\xi}}$ and $\hat{\theta}$ — $\hat{\dot{\eta}}$ and $\hat{\theta}$

(d)   — $\hat{\dot{\xi}}$ and $\hat{\dot{\theta}}$ — $\hat{\dot{\eta}}$ and $\hat{\dot{\theta}}$
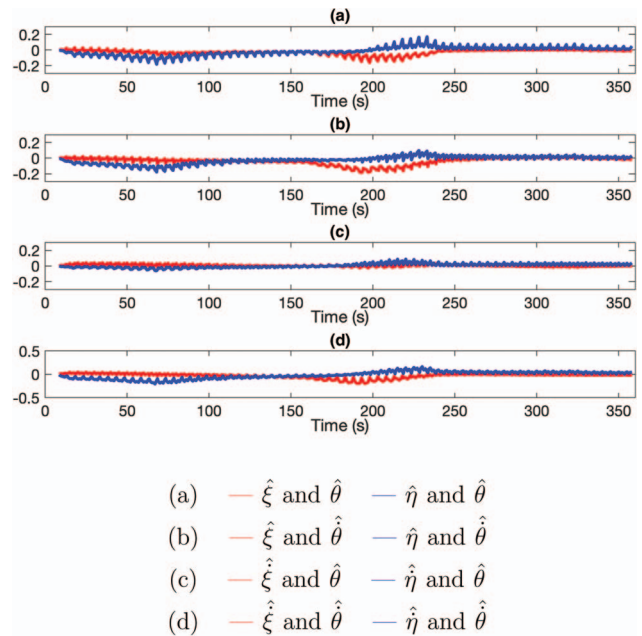
Fig. 11.   Cross-correlation coefficients between the elements from two state vectors.

results from a scenario with one passive tracker and one active tracker show the performance of heterogeneous T2TF with cross-covariance. It can be seen that with the cross-covariance, the T2TF can achieve improved performance with lower RMSE and better statistical efficiency. The cross-correlation coefficients are sometimes positive and sometimes negative, which confirms the results obtain in [3] through an MC investigation.

REFERENCES

[1]   Y. Bar-Shalom, P. Willett, and X. Tian
       Tracking and Data Fusion. Storrs, CT: YBS Publishing, 2011.

[2]   X. Tian and Y. Bar-Shalom,
       "On Algorithms for Asynchronous Track-to-Track Fusion,"
       in *Proc. Int. Conf. Inf. Fusion*, Edinburgh, UK, July 2010.

[3]   T. Yuan, Y. Bar-Shalom, and X. Tian
       "Heterogeneous Track-to-Track Fusion,"
       J. Adv. Inf. Fusion, vol. 6, no. 2, pp. 131–149, Dec. 2011.

[4]   M. Mallick, K. C. Chang, S. Arulampalam, and Y. Yan,
       "Heterogeneous Track-to-Track Fusion in 3D Using IRST
       Sensor and Air MTI Radar," *IEEE Trans. on Aerospace
       Engineering Systems*, vol. 55, no. 6, pp. 3062–3079, Dec. 2019

[5]   Y. Bar-Shalom, X. R. Li, and T. Kirubarajan
       *Estimation with Applications to Tracking and Navigation:
       Theory, Algorithms and Software*. New York: Wiley, 2001.

[6]   K. Yang, Y. Bar-Shalom, and P. Willett,
       "Track-to-Track Fusion with Crosscovariances from Radar
       and IR/EO Sensor," in *Proc. Int. Conf. Inf. Fusion*, Ottawa,
       Canada, July 2019.

[7]   M. R. Morelande and N. J. Gordon
       "Target Tracking Through a Coordinated Turn," in *Proc.
       IEEE Int. Conf. Acoust., Speech, and Signal Process.
       (ICASSP '05)*, 2005, vol. 4, pp. iv/21–iv/24.
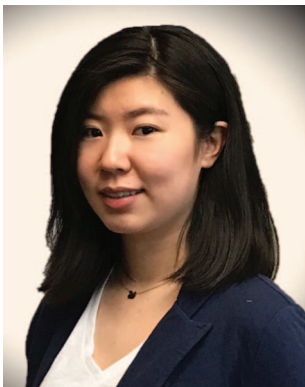
Kaipei Yang received the B.S. degree from the Northwestern Polytechnical University, Xi'an, China, in 2014, and the Ph.D. degree from the University of Connecticut, Storrs, CT, USA, in 2019. She is currently an Assistant Research Professor with the Department of Electrical and Computer Engineering, University of Connecticut. Her research interests include statistical signal processing, estimation theory, and information fusion. She gained experience in autonomous driving vehicles while working at NIO, San Jose, CA, USA, in 2018.

Yaakov Bar-Shalom received the B.S. and M.S. degrees in electrical engineering from the Technion, Haifa, Israel, in 1963 and 1967, respectively, and the Ph.D. degree in electrical engineering from Princeton University, Princeton, NJ, USA, in 1970. From 1970 to 1976, he was with Systems Control, Inc., Palo Alto, CA, USA. He is currently a Board of Trustees Distinguished Professor with the Department of Electrical and Computer Engineering and Marianne E. Klewin Professor in Engineering with the University of Connecticut, Storrs, CT, USA. His current research interests include estimation theory, target tracking, and data fusion. He has authored or coauthored more than 550 papers and book chapters, and coauthored/edited 8 books, including *Tracking and Data Fusion* (YBS Publishing, 2011). He has been elected Fellow of IEEE for "contributions to the theory of stochastic systems and of multitarget tracking." He was an Associate Editor for the *IEEE Transactions on Automatic Control and Automatica*. He was General Chairman of the 1985 ACC, Chairman of the Conference Activities Board of the IEEE CSS and member of its Board of Governors, General Chairman of FUSION 2000, President of ISIF in 2000 and 2002, and Vice President for Publications during 2004–2013. In 1987, he was the recipient of the IEEE CSS Distinguished Member Award. Since 1995, he is a Distinguished Lecturer of the IEEE Aerospace and Electronic Systems Society. He was the corecipient of the M. Barry Carlton Award for the best paper in the *IEEE Transactions on Aerospace and Electronic Systems* in 1995 and 2000. In 2002, he was the recipient of the J. Mignona Data Fusion Award from the DoD JDL Data Fusion Group. He is a member of the Connecticut Academy of Science and Engineering. In 2008, he was the recipient of the IEEE Dennis J. Picard Medal for Radar Technologies and Applications, and in 2012 the Connecticut Medal of Technology. He has been listed by academic.research.microsoft (top authors in engineering) as #1 among the researchers in aerospace engineering based on the citations of his work. He was the recipient of the 2015 ISIF Award for a Lifetime of Excellence in Information Fusion. This award has been renamed in 2016 as the Yaakov Bar-Shalom Award for a Lifetime of Excellence in Information Fusion.

Peter Willett received the B.A.Sc. (engineering science) degree from the University of Toronto, Toronto, Canada, in 1982, and the Ph.D. degree from Princeton University, Princeton, NJ, USA, in 1986. He has been a faculty member with the Department of Electrical and Computer Engineering, University of Connecticut, Storrs, CT, USA, since 1986. Since 1998, he has been a Professor, and since 2003 an IEEE Fellow. His primary areas of research include statistical signal processing, detection, machine learning, communications, data fusion, and tracking. He has authored or coauthored more than 650 papers on these topics. He was Editor-in-Chief for the *IEEE Signal Processing Letters* from 2014 to 2016. He was Editor-in-Chief for the *IEEE Transactions on Aerospace and Electronic Systems* from 2006 to 2011, and then AESS Vice President for Publications (2012–2014). He was a member of the IEEE AESS Board of Governors (2005–2010, 2011–2016) and of the IEEE Signal Processing Society's Sensor-Array and Multichannel (SAM) technical committee (and Chair 2015–2016).